WILLARD J. PIERSON, JR.

SOME APPROACHES FOR COMPARING REMOTE AND IN-SITU ESTIMATES OF DIRECTIONAL WAVE SPECTRA

Radar imaging systems inherently measure different properties of the spectrum than do the more traditional directional wave buoys. Analysis of the present methods of measuring heave acceleration, pitch, and roll on buoys under development by the National Data Buoy Center (NDBC) explains some of the inconsistencies that have been found not only for NDBC buoys but also for other directional wave buoys. The methods used for buoys can be extended to airborne and spaceborne systems in order to compare spectra estimated by the different systems.

INTRODUCTION

Ways to measure the rise and fall of the sea surface caused by passing waves as a function of time, $\xi(t)$, have been developed over the past few decades. The estimation of the frequency spectrum in the form $\hat{S}(f)$ or $\hat{S}(\omega)$ has become routine. (The circumflexes indicate spectral estimates.) Donelan and Pierson[1] have shown that the sampling variability of estimates of frequency spectra of wind-generated waves can be described, more or less, by the available theories that represent waves as a linear quasi-stationary (in a time series sense) Gaussian process.

Four methods are available for estimating the directional spectrum of deep-water waves, in which the sea surface is represented by $\xi(x,y,t)$. The methods depend approximately on the assumption for deep water that the waves are a linear superposition of sinusoids that are freely propagating linear waves in deep water, i.e., that

$$k = \omega^2/g \, . \tag{1}$$

The first of the four methods is the one being developed for operational use as described by Steele et al.[2] for the National Data Buoy Center (NDBC) program. It has a lengthy history and is based on the theory described by Longuet-Higgins et al.[3] For current operational use, the end product of the measurements of heave acceleration, pitch, and roll as a function of time at a fixed point is a partial description of the directional spectrum, Eq. 2, such that the frequency-dependent quantities, $\hat{A}_1$, $\hat{\theta}_1$, $\hat{A}_2$, and $\hat{\theta}_2$, estimate the first two terms of the angular spread in the direction of travel of the spectral components.

$$\hat{S}(f,\theta) = \hat{S}(f_i) \, \frac{1}{\pi} \left\{ \frac{1}{2} + \hat{A}_1(f_i) \cos[\theta - \hat{\theta}_1(f_i)] + \hat{A}_2(f_i) \cos 2[\theta - \hat{\theta}_2(f_i)] \right\} . \tag{2}$$

Both $\hat{S}(f_i)$ for a simple frequency measurement and $\hat{S}(f_i,\theta)$ are estimated at a discrete set of frequencies, $f_i = i/T$, where, say, $T = 100$ seconds and i ranges from 0 to 50. A large buoy filters out the waves above about 0.3 hertz so that only five numbers (or estimates) for about 30 frequency bands describe the waves for this method of measurement and analysis.

The complete expression for Eq. 2 would require the determination of all of the higher harmonics of the angular spreading function, $\hat{D}(f_i,\theta_i)$, in the braces of Eq. 2, i.e.,

$$\hat{D}(f_i,\theta_i) = \frac{1}{\pi} \left[\frac{1}{2} + \sum_{n=1}^{\infty} \hat{A}_n(f_i) \cos(n(\theta - \hat{\theta}_n(f_i))) \right] . \tag{3}$$

The second of the four methods, the surface contour radar, is described by Walsh et al.[4] (and by Walsh et al. elsewhere in this issue). It comes the closest to measuring the function $\xi(x,y)$ at an instant of time from an aircraft. Ingenious ways to account for the aircraft velocity vector and the moving waves have been developed that eliminate the false part of the spectral estimates. In this system, the spectral estimates are of the form, $\hat{S}(k_x,k_y)[dk_x \, dk_y]$, where in a linear system

$$k_x = \frac{\omega^2}{g} \cos\theta, \; k_y = \frac{\omega^2}{g} \sin\theta \, . \tag{4}$$

Willard J. Pierson, Jr., is a professor at the Institute of Marine and Atmospheric Sciences, the City College of the City University of New York 10031.

The radar ocean-wave spectrometer, the third of the four methods, is described by Jackson et al.[5,6] and also by Jackson in this issue. It scans in a circle as an aircraft flies along and filters out waves traveling at an angle to the direction of the scan. The quantity actually measured is a filtered version of $\partial\xi/\partial r$ in polar coordinates, and the spectral estimate that is recovered is of the form $\hat{S}(k,\theta)[k\ d\theta\ dk]$.

The last of the four methods is described by Beal et al.[7] and also by Monaldo elsewhere in this issue. This technique uses data from a synthetic aperture radar approximately of the form $\partial\xi(x,y)/\partial x$, where x is perpendicular to either an aircraft flight line or a spacecraft flight line. A spectrum of the form $\hat{S}(k_x,k_y)\ [dk_x\ dk_y]$ is recovered. The method does not do as well for high wavenumbers in the direction of the flight line that are still of importance in defining the elevation spectrum.

To validate the aircraft and aircraft/spacecraft systems described above, the wavenumber spectra obtained have been transformed to estimates of $\hat{S}_R(f)$ and compared to estimates of $\hat{S}_B(f)$ (where R means remote, for aircraft or spacecraft, and B means buoy). Walsh has compared the spectral estimates obtained by means of the surface contour radar with the Cartwright[8] angular spreading function and the coefficients in Eq. 2. Comparisons of the aircraft and spacecraft systems without the aid of buoy data were also made.

Spectral estimates have an uncertainty that can be described in terms of a number defining the degrees of freedom of the estimate for the chi-square distribution. There is an inherent uncertainty in a spectral estimate that must be considered in using spectra and in comparing different spectra. An apparent advantage of remote sensing systems is that the spectral estimates appear to have many more degrees of freedom and consequently are closer to the "true" value of the spectrum than are spectra obtained from time histories at a point or points. It takes a while for the waves to go past a point or an array of points, whereas they are present on the entire surface at any moment.

THEORETICAL AND ANALYTICAL QUESTIONS

Ocean waves are, in fact, not linear and Eq. 1 is, in fact, an approximation. Ocean waves break; linear waves cannot. A better equation to enable Eq. 1 to go back and forth between vector wavenumber **k** and circular frequency ω is not immediately obvious, especially in terms of mapping $\hat{S}(\omega,\theta)$ into either $\hat{S}(k,\theta)$ or $\hat{S}(k_x,k_y)$, although some of the studies of Mitsuyasu and his colleagues (for example, Mitsuyasu et al.[9]) and Donelan et al.[10] and other research in progress may be potentially applicable.

Moreover, for its present stage of development, the NDBC data at times yield values of $\hat{A}_1(f_1)$ and $\hat{A}_2(f_1)$ in Eq. 2 that are greater than 1. The data also suggest a problem with what has been interpreted as increasing "noise" at frequencies in the spectral estimates where a linear theory would not indicate any spectral activity, as shown in Steele et al.[2] (see their Fig. 5 and associated text). It can be shown that every coefficient in Eq. 3, which includes $\hat{A}_1(f_1)$ and $\hat{A}_2(f_1)$ in Eq. 2, must be less than 1, since $D(f,\theta)$ for any f must be everywhere positive and have the property, by definition, that

$$\int_{-\pi}^{\pi} D(f,\theta)\ d\theta = 1\ . \tag{5}$$

NDBC is investigating the need to obtain 10-minute vector averages of the wind speed and direction continuously, except for one 8-minute average each hour to permit data transmission. There are no technological difficulties in doing this. These would be the only available data of sufficient quality to validate remote sensing systems that are planned to describe the wind.

In the same sense, aircraft and spacecraft systems to measure directional wave spectra will need to be validated against in-situ spectral estimates from NDBC or other buoys that can provide spectra either in the form of Eq. 2 or in an improved form following the results of Long and Hasselmann[11] and Long.[12] Remote sensing systems and in-situ systems for measuring winds and waves are not competitive; in fact, they are complementary. Information from the combined systems is greater than the information from either system alone.

A MODEL

To compare wave frequency and wavenumber spectra, a model for the sea surface is needed. One possible model for a linear theory is given in Neumann and Pierson[13] (page 339). An equivalent model that better illustrates some of the features of the analysis methods presently in use assumes that the variance spectrum, $S(\omega,\theta)$, for which derivatives exist for both ω and θ, is zero below some frequency, $\omega_{\min}$, and above some frequency, ω_{Nyquist}, because of the instrument's characteristics.

Then let

$$m_{ij} = \int_{\theta_j-\Delta\theta/2}^{\theta_j+\Delta\theta/2} \int_{\omega_i-\Delta\omega/2}^{\omega_i+\Delta\omega/2} S(\omega,\theta)d\theta \tag{6}$$

and form

$$a_{ij} = R_1(m_{ij})^{1/2} \tag{7}$$

and

$$b_{ij} = R_2(m_{ij})^{1/2}\ , \tag{8}$$

where R_1 and R_2 are numbers drawn at random from a normal probability density function with a zero mean and a unit variance. With, say, $\omega_1 - \Delta\omega/2 = \omega_{\min}$, $\omega_p + \Delta\omega/2 = \omega_{\text{Nyquist}}$, and with $\theta_1 - \Delta\omega/2 = -\pi$ and $\theta_q + \Delta\theta/2 = \pi$ as $\Delta\omega$ and $\Delta\theta$ become small and p and q become very large, the sea surface for a linear model can be represented by Eq. 9:

$$\xi(x,y,t) =$$

$$\sum_i \sum_j a_{ij} \cos\left(\frac{\omega_i^2}{g}(\cos\theta_j x + \sin\theta_j y) - \omega_i t\right) + b_{ij} \sin\left(\frac{\omega_i^2}{g}(\cos\theta_j x + \sin\theta_j y) - \omega_i t\right). \quad (9)$$

This model occupies the entire domain $-\infty < t < \infty$, $-\infty < x < \infty$, and $-\infty < y < \infty$, which is, of course, unrealistic because the spectrum of the waves changes from one place on the ocean to another at any time and with time at any place on the ocean. Waves in a poorly defined sense are an evolutive random process, and it is necessary to assume that the observations that are obtained can be represented by something like Eq. 9 for analytical purposes.

From Eq. 9, two derivatives can be computed as $\partial\xi(x,y,t)/\partial x$ and $\partial\xi(x,y,t)/\partial y$. A data buoy thus obtains simultaneous time histories of the form $\xi(0,0,t)$, $\partial\xi(0,0,t)/\partial x$, and $\partial\xi(0,0,t)/\partial y$ since the exact location of the buoy is not relevant. Also from Eq. 9, the airborne system of Walsh et al.[4] and the various synthetic aperture radars obtain data essentially of the form $\xi(x,y,0)$ or $\partial\xi(x,y,0)/\partial x$.

The three functions of time defined above represent a three-component vector Gaussian process with three variance spectra, three cospectra, and three quadrature spectra, as defined, for example, in Steele et al.[2] and as based on the original work of Longuet-Higgins et al.[3] and Cartwright.[8] The resulting nine components are usually designated $S(\omega)$, $C_{22}(\omega)$, $C_{33}(\omega)$, $C_{12}(\omega) \equiv 0$, $Q_{12}(\omega)$, $C_{13}(\omega)$, $Q_{13}(\omega)$, $C_{23}(\omega)$, and $Q_{23}(\omega) \equiv 0$.

THE SAMPLE AND THE ESTIMATES

For buoy data, the Nyquist frequency is well below 0.5 hertz so that the data can be sampled with a Δt of 1 second to obtain a sample of a vector process of the form $\xi(0)$, $\xi(p\Delta t)$ ... $\xi[(N-1)\Delta t]$, $\xi_x(0)$ ... $\xi_x[(N-1)\Delta t)]$, $\xi_y(0)$ ... $\xi[(N-1)\Delta t)]$. There is an obvious extension to x,y space for two of the remote systems described in the introduction.

The $3N$ numbers representing the buoy data then need to be processed to obtain *estimates* of the functions of frequency defined above as in $\hat{S}(\omega)$, $\hat{C}_{22}(\omega)$, and so on. There is a parallel extension of these concepts for the analysis, for example, of $\xi(x,y,0)$. Depending on the state of the available theories for the analysis of vector time series, buoy data have been analyzed by at least two primarily different methods so as to estimate the spectra and cross spectra. A third method is now technologically possible. From these estimates of the spectra and cross spectra, there are, in turn, two different ways to estimate the quantities $\hat{A}_1$, $\hat{A}_2$, $\hat{\theta}_1$, $\hat{\theta}_2$ in Eq. 2.

The first method would be to use the theory described by Tukey,[14] as extended to cross spectra and as described in detail in Blackman and Tukey.[15] This method will not be discussed, but its use in this particular application or for the study of $\xi(x,y)$ probably introduces some rather strange effects in the spectral estimates. The second method is the one described by Harris.[16] It was used for the analysis of the buoy data in Steele (personal communication, 1985). The third method would be to apply the concepts in Harris[16] to the analysis of all the $3N$ data values, as described below, perhaps with further refinements. This method has become practical only recently because of the greater speed and memory of microcomputers. It is not at all difficult, using the algorithms described in Cooley and Tukey,[17] for example, to do a Fourier transform of, say, 10,000 data points equally spaced in time by means of the fast Fourier transform.

THE HARRIS METHOD

To simplify this discussion, a given sample size of 1000 data points 1 second apart for ξ, $\partial\xi/\partial x$, and $\partial\xi/\partial y$ will be assumed. Note that not only have the data been sampled only at $n\Delta t$ but also that the sample has been acted on so that a much longer series of values has been set to zero outside of a boxcar data window $w(t) = 1$ for $0 \le n\Delta t \le (N-1)\Delta t$.

The Harris method consists of breaking up the large sample of, say, 1000 ($\times$ 3) values into smaller samples of 100 values and, as in Steele's analysis (personal communication, 1985), perhaps using 100 value subsamples overlapping by 50 values, i.e., points 0 to 99, 50 to 149, and so on. Each sample is jagged at the end points, and the first and last points usually form a jump discontinuity.

To improve the analysis, Harris[16] describes about 23 data windows by which the 100-point samples in the time domain can be multiplied so as to attempt to improve the spectral estimates. Those that have been tried at NDBC are the parabolic window $P(t)$ and the cosine-squared window $C2(t)$ such that the three components of the vector process are each multiplied by either Eq. 10 or 11, where the constants A and B normalize the window:

$$P(t) = A\{1 - [t/(T/2)]^2\}, \quad (10)$$

$$C2(t) = B(\cos 2\pi t/2T)^2 \quad (11)$$

(for $-T/2 < t < T/2$, where $T = 50$ seconds).

The Fourier transforms of each subsample are then processed to yield estimates of the spectra and cross spectra at a resolution of 0.01 hertz at the frequencies $p/100$, where p varies from 0 to 50. The 19 subsamples are then pooled at each frequency to obtain the final estimates of the spectra and cross spectra.

The original method of Longuet-Higgins et al.[3] recovers quantities that in turn yield $\hat{A}_1$, $\hat{\theta}_1$, $\hat{A}_2$, and $\hat{\theta}_2$ from equations such as Eqs. 12 and 13, since $A_1 \cos(\theta - \hat{\theta}) = \hat{a}_1 \cos\theta + \hat{b}_1 \sin\theta$:

$$\hat{a}_1(p/100) = g\,\hat{Q}_{12}(p/100)\,[(100)^2/4\pi^3 p^2], \quad (12)$$

$$\hat{a}_2(p/100) = g^2\,(\hat{C}_{22}(p/100) - \hat{C}_{33}(p/100)) \times [(100)^4/16\pi^5 p^4], \quad (13)$$

and so on, for $\hat{b}_1(p/100)$ and $\hat{b}_2(p/100)$.

From Eq. 1, this is equivalent to multiplying the estimates at $\omega_p = 2\pi p/100$ by $(\pi k_p)^{-1}$ and $(\pi/k_p^2)^{-1}$, where $k_p = (2\pi p/100)^2/g$.

Long[12] has proposed an alternative method for recovering the same quantities:

$$\hat{a}_1 = \hat{Q}_{21}\,[\hat{S}_{11}\,(\hat{C}_{22} + \hat{C}_{33})^{-1/2}]\,, \qquad (14)$$

$$\hat{a}_2 = (\hat{C}_{22} - \hat{C}_{33})\,(\hat{C}_{22} + \hat{C}_{33})^{-1} \qquad (15)$$

(and so on for the other quantities). These do not need to be multiplied by the values of k at the resolved frequencies.

If both the method of spectral estimation and the linear model are correct, the quantity

$$R = \frac{\omega_p^2}{g}\,\hat{S}(\hat{C}_{22} + \hat{C}_{33})^{-1/2} \qquad (16)$$

ought to be equal to 1.

A HIGH-RESOLUTION ANALYSIS

In contrast to the Harris procedure, the original three-component vector process could be analyzed as a single time series at a resolution of 0.001 hertz or as $p/1000$ as p varies from 0 to 500, either with a boxcar data window or perhaps with some more appropriate data window. The sum over frequency, for example,

$$\hat{S}(q/100) = \frac{1}{11}\sum_{p=q-5}^{q+5}\hat{S}(p/1000)\,, \qquad (17)$$

would then define the spectrum at a resolution of 0.01 hertz with 22 degrees of freedom. Similar operations would define the cross spectra and the quantities in Eq. 2 by means of an interpretation by Goodman.[18]

Donelan and Pierson[1] have done this analysis for elevation time histories alone with a boxcar data window and a resolution of $p/1024$ hertz ($p = 0$ to 512). The results that would be predicted for a stationary Gaussian process were verified, and the high degree of sampling variability from one time history to another was demonstrated.

EXAMPLES

From the limiting process defined earlier, the coefficients in Eq. 9 are infinitely dense (except where the spectrum is zero) over the frequency axis, and care must be taken in interpreting the summations over j. For the time series $\xi(0,0,p\Delta t)$, the Harris method and the higher resolution method can be compared by letting $\Delta\omega$ or Δf be finite but small. Figure 1 illustrates the high-resolution results for a boxcar data window applied to a narrow band of swell extending from about 0.037 to 0.043 hertz.

Data windows in the time domain produce spectral windows (the writer prefers to use the term spectral filters) in the frequency domain, and, for a 0.001-hertz

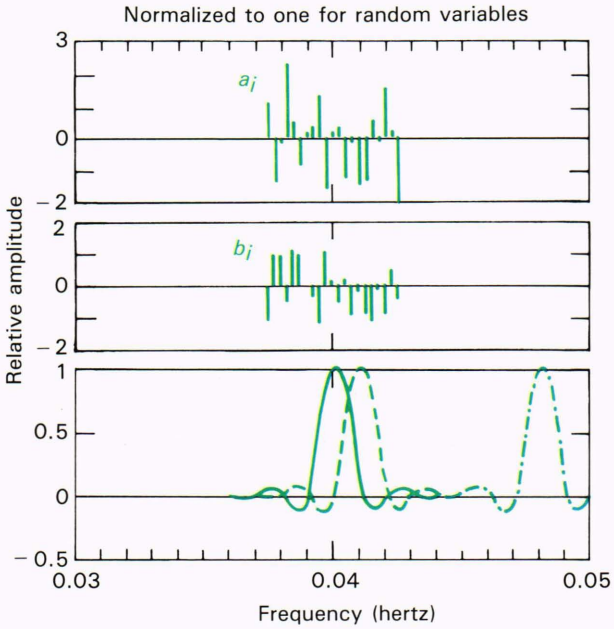

Figure 1—Example of high-resolution frequency filters to illustrate their effects on an evenly, more highly resolved, narrow band of swell (see text).

resolution, the spectral filter for the boxcar data window is given approximately by the solid curve in Fig. 1 for the value that would be recovered for the Fourier coefficients in the Fourier transform at a frequency of 0.04 hertz. This function is often called the sine-cardinal function. For example, the value of $\hat{a}(40/1000)$ is recovered by multiplying each of the spikes for a_i^* by the value of the solid curve and summing the values. For the example, the a_i^* are numbers drawn at random from a unit-normal zero-mean Gaussian distribution. This weighted sum would be a zero-mean normally distributed variable with a variance given approximately (because of leakage in the spectral filter) by

$$\int_{0.0395}^{0.0405} S(f)\,df\,.$$

Also, $\hat{b}(40/1000)$ would be found from a similar operation on the $\hat{b}_i$. The variance spectrum is then estimated:

$$\hat{S}(40/1000) = (\hat{a}^2 + \hat{b}^2)/2\,. \qquad (18)$$

(See Donelan and Pierson[1] for further details.) The spectral filters for 0.041 and 0.048 hertz are illustrated in Fig. 1 by the dashed and dot-dashed curves, respectively.

To understand the full effect of a resolution of 0.001 hertz, the solid curve in Fig. 1 should be considered to be located sequentially at each tick mark on the frequency axis. In each position, the values of the spectral filter multiply the values of the a_i^*, and the values are summed. The result is the cosine Fourier component of

a discretized Fourier analysis for the frequency on which the filter is centered. Similar results are found for the sine coefficients. There is some overlap in the use of the a_i^* and b_i^* from 0.036 to 0.044 hertz. The Fourier coefficients are very small for frequencies below 0.035 hertz and above 0.045 hertz. The postulated narrow band of swell is well resolved. For historical interest, see Munk.[19]

Figure 2 illustrates the Harris method of analysis for boxcar, parabolic, and cosine-squared data windows at a frequency resolution of $p/100$ hertz as p varies from 0 to 50. Only frequencies from 0.02 to 0.07 are shown. A hypothetical narrow band of swell is illustrated between 0.04 and 0.05 hertz at a high resolution along with the start of a hypothetical wind-wave spectrum, except that the values for the wind-wave spectrum might need to be six times higher at the start, tapering off slowly toward higher frequencies. The various spectral filters can now be centered sequentially only over the frequencies shown by the ticks on the frequency axis.

The 100-point samples with a boxcar data window broaden the spectral filter by a factor of 10, with first zeros at 0.03 and 0.05, instead of at 0.039 and 0.041 as for a 1000-point sample, for a center frequency of 0.04, for example. The other windows put the first zeros even farther from the frequency at which the estimate is supposed to apply.

The estimates with the filters shifted to 0.03 hertz include terms from the band of swell between 0.04 and 0.05 hertz. Yet, for the example, there is nothing in the spectrum actually between 0.025 and 0.035 hertz.

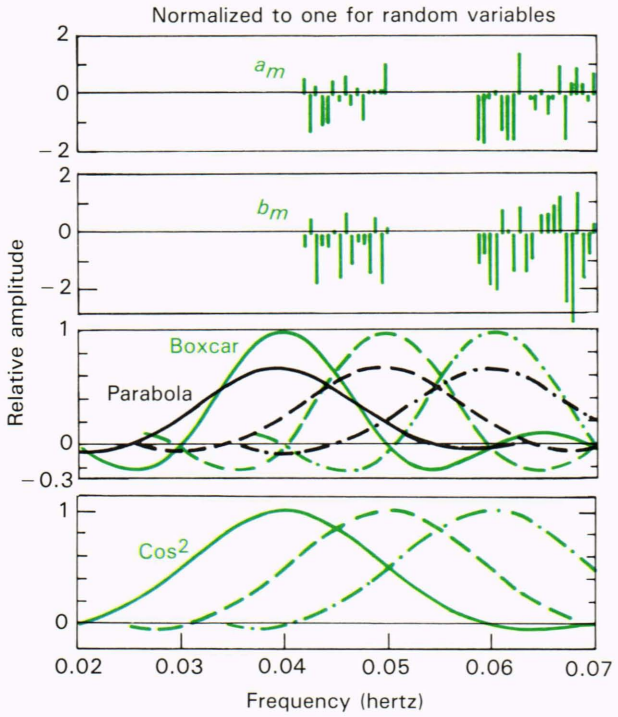

Figure 2—Examples of the effects of coarse resolution frequency filters from three different data windows to illustrate their effects on a narrow band of swell and the lower frequencies in wind sea (see text).

All three filters yield a value for 0.04 hertz, but nothing is there in the example at 0.04 hertz. The boxcar filter picks up the start of the more highly resolved values near 0.06 hertz and produces a value at 0.04 hertz that is somewhat too large for an average over many Monte Carlo simulations of the model.

At 0.05 hertz, all three filters mix up the sea and the swell. Because the spectrum of the sea is higher, the terms that contribute to 0.05 hertz could dominate the swell even though weighted by a smaller number by the frequency filter.

At 0.06 hertz, the spectral filters begin to respond to the high-frequency part of the modeled waves, but a good portion of the band of swell between 0.04 and 0.05 hertz is still included in the Fourier coefficient that represents conditions at 0.06 hertz.

For this example, and undoubtedly for actual conditions, a 100-second sample operated on by either a parabolic window or a cosine-squared window would mislocate contributions from the true, but unknown, wave spectrum by ± 0.02 hertz at each frequency band that is resolved by a 100-point fast Fourier transform. For this example, values would be recovered at 0.03 hertz, whereas nothing is there. At 0.04 hertz there would be values, whereas nothing actually exists until slightly higher frequencies. The values at 0.05 hertz are contaminated by 0.06 hertz. The gap between 0.05 and 0.06 hertz never shows up. The values at 0.06 hertz are contaminated by values between 0.04 and 0.05 hertz. Clearly, the spectral bands have not been resolved to within ± 0.005 hertz.

A spectrum estimated by the above method, using one of the windows above, is shown in Fig. 3 along with the estimates of the wave direction. Clearly the low-frequency swell from 0.05 to 0.09 hertz is traveling in a different direction from the high-frequency wind sea. The spectral estimates can be interpreted by considering the effects of the parabolic and cosine-squared data window and the corresponding spectral filters.

Spectra analyzed this way have to be interpreted cautiously. The values are plotted at 0.01-hertz intervals. Each point in the plot is influenced by frequencies in the "true" spectrum as much as ± 0.02 hertz away.

The lowest point appears to be 0 at 0.02 hertz. There may have been nothing in the "true" spectrum at 0.03 and 0.04 hertz. The value at 0.04 hertz may have come from 0.06 and 0.07 hertz. The value at 0.06 hertz (as well as at 0.07, 0.08, and, perhaps, 0.09 hertz) may have been the first band that would have contained a part of the "true" spectrum at a higher resolution. The values at 0.10, 0.11, and 0.12 hertz may really be 0, with the spectral filter including the lower frequency swell in the calculation for 0.10 hertz, both sea and swell being included at 0.11 hertz, and the sea being included at 0.12 hertz. A 1000-point fast Fourier transform could easily resolve a possible on/off property of the swell and locate the start of the wind-sea spectrum.

The situation becomes even worse as soon as pitch and roll spectral estimates and spectra and cross spectra become involved. There are spectral estimates at some frequencies for which there is actually no contribution at

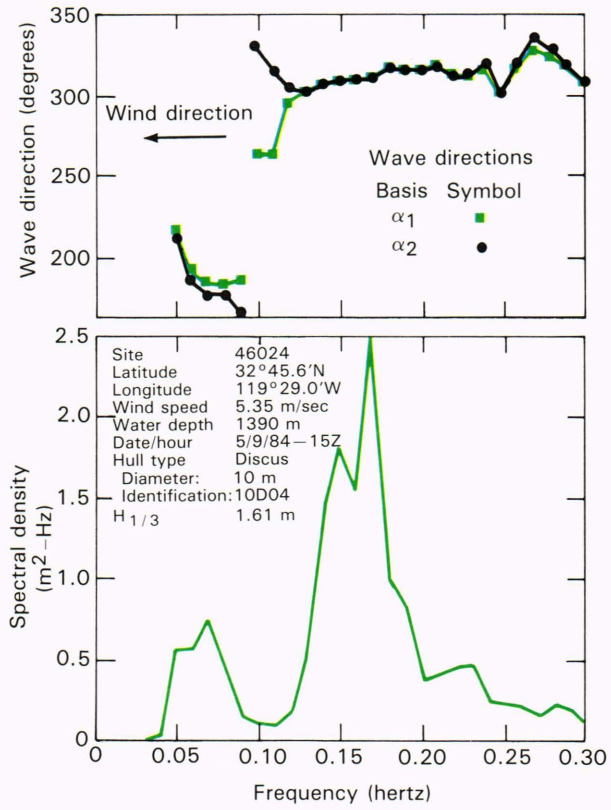

Figure 3—Sea plus swell spectral estimates and direction of travel (from Fig. 8 of Ref. 2).

those frequencies from the true spectrum. Actual frequency components in the true spectrum are not centered at the frequency of the estimated spectrum. Frequencies from as far away as ± 0.02 hertz are in the sum that determines the spectral estimate for a given frequency.

The computation of the quantities needed in Eqs. 2, 12, and 13 requires that various spectral estimates be divided by either ω^2/g or ω^4/g^2. The coefficients for, say, 0.04 hertz are contaminated by contributions of an unknown amount (usually) from 0.06 hertz. If the contributions from 0.06 hertz as computed from the analysis procedure were actually at 0.04 hertz, one should really have divided by 3.6×10^{-4} instead of by 1.6×10^{-4} (each multiplied by $(2\pi)^2/g$), with even larger differences for k^2. In the extreme, large errors are possible at low frequencies. The unknown error is, of course, somewhat less and is a function of the true but unknown spectrum.

Presently available frequency spectra of ocean-wave time histories that resolve the total variance into frequency bands at various resolutions appear to have the general property for a linear model that there is a sharp rise beginning at some low frequency to a poorly defined spectral peak (see Pierson[20]), followed by a more gradual decrease toward low values at the high-frequency part of the spectrum. The overall shape of the spectrum has been smoothed somehow by weighted averages over some band of more highly resolved frequency bands. These bands disguise the extreme variability of the spectral estimates that would have been obtained by a Fourier transform at its maximum resolution having a chi-square distribution with two degrees of freedom.

As wind seas grow with increasing wind speed toward lower frequencies, the present method of buoy analysis at NDBC puts these frequencies at 0.03 hertz and can help explain the increase in noise level found by Steele et al.[2] at the low frequencies.

For this coarse resolution and using the Harris method, neither the method originally proposed by Longuet-Higgins et al.[3] nor the more recent Long[12] method can provide reliable estimates of $\hat{A}_1(f_i)$ and $\hat{A}_2(f_i)$ in Eq. 2. For example, the earlier method gives values of $\hat{A}_1(f_i)$ and $\hat{A}_2(f_i)$ that are greater than 1 if the true spectrum has values above $f_i = p/100$, but none below it, and a frequency of $p/100$ is used to calculate the wavenumber. Similarly, the Long method typically gives values of R in Eq. 16 that are less than 1 below the spectral peak and greater than 1 above the spectral peak. A report by Barstow et al.[21] shows this effect. The result is an artifact of the analysis method and not proof that Eq. 1 is inapplicable. Other analyses for wind waves as in Donelan et al.[10] show that the phase speed is closely related to the linear value and thus that Eq. 1 is fairly accurate.

THE DIRECTIONAL SPREAD

The estimates of $\hat{A}_1$ and $\hat{A}_2$ in Eq. 2 have been used in an attempt to define the full angular spreading function as in Eq. 3 by assuming various functional forms for $D(f,\theta)$. A coarse frequency-resolution analysis of buoy data will usually not provide unbiased estimates of $\hat{A}_1$ and $\hat{A}_2$, no matter which estimation method is used. The angular spreading functions that have been obtained result in part from the systematic biases in the estimates. The situation becomes even worse in attempting to analyze cloverleaf buoy data as in Mitsuyasu et al.[22] since calculations involving k^3 and k^4 are involved.

NONLINEAR WAVE PROPERTIES

The analysis methods described above result in a strange paradox. Theories and analysis methods based on a linear model for the waves seem to work fairly well after a fashion. Yet a wind-generated sea is clearly about as nonlinear as waves can be. Artifacts in the estimation of wave spectra appear to mask the true nonlinear properties of waves. Those artifacts need to be eliminated, and we must find ways to study the nonlinear properties of waves at sea.

ADDITIONAL CONSIDERATIONS

Even for simple spectra, the same data can be processed in different ways to obtain a wide range of spectral estimates, which, at successive frequencies, may or may not be independent in the probability sense.

It is often difficult to determine the details of the procedure used to estimate a particular spectrum and the characteristics of the frequency-smoothing filter that were used to increase the degrees of freedom at each frequency of the estimated spectrum at the expense of reso-

lution. The confidence intervals for the estimated significant wave height are also difficult to determine.

At a conference many years ago, a speaker compared high-resolution and low-resolution spectral estimates of swell. The estimates were quite different, and the speaker concluded that using spectra was not a good way to study waves. At another conference, a speaker claimed to have developed a different way to recover spectra from records $T/2$ seconds long that had the same properties as spectra from records that were T seconds long. Neither speaker was correct. For a given sample, high resolution can only be obtained at the expense of increased sampling variability. Conversely, sampling variability can be reduced only at the expense of high resolution.[15] Spectral filters are involved in such a way that different values can be obtained for the spectral estimates, even at the same resolution.

In order to compare spectra estimated from data from the aircraft and spacecraft systems described in the beginning of this paper with each other and with spectra estimated from buoy data, the details of the spectral estimation procedure must be provided for each system.

The transformation of wavenumber spectra, obtained in either Cartesian or polar form, to frequency-direction spectra, even for a linear model, is not simple. Knowledge is needed of the combined effect of the two-dimensional spectral filters that were involved in both data recording and data processing.

It is possible for the two spectra being compared to appear to disagree with each other and yet actually to have been correct insofar as their interpretation in terms of the spectral filters that were applied is concerned.

Buoy data do not provide all the information needed to estimate all the properties of a directional spectrum. They can keep track of some features of how the waves are changing at, perhaps, half-hour intervals continuously. The spectra are always available for comparison with other kinds of spectra.

The smaller the angular spread, the larger the number of terms in the Fourier series needed to come close to approximating the angular spreading function. For an angular width of 20 degrees, or $\pi/18$ radians, the first few Fourier coefficients at a fixed frequency in Eq. 3 are approximately in proportion to 0.9949, 0.9790, 0.9549, 0.9207, and so on to the eighteenth harmonic, which is zero, and so on to negative values.

There are at least two ways to compare spectral values provided by a buoy with spectral values from one of the other systems. One can transform the wavenumber spectra from the second system into an appropriate form that would allow a direct comparison, frequency by frequency, with the buoy data, as in Eq. 2. There is no need either to postulate some form of the angular spreading function or to require that the square bracket in Eq. 2 be positive everywhere. The sampling variability of the terms in the square bracket of Eq. 2 needs to be better understood.

Second, one can make sure that the buoy data are reported in a form amenable to the application of the theoretical results of Long and Hasselmann[11] and Lawson and Long.[23] The use of the "minimum nastiness" method requires a "first guess" input for the angular spread at each frequency. That input could be the estimated form of the angular spreading function from the aircraft or spacecraft system. The buoy data could then be used iteratively as a check. The use of this "bootstrap" method would require additional study before implementation, but it could be very powerful.

REFERENCES

[1] M. A. Donelan and W. J. Pierson, "The Sampling Variability of Estimates of Spectra of Wind-Generated Gravity Waves," *J. Geophys. Res.* **88**, 4381-4392 (1983).

[2] K. E. Steele, J. C. K. Lau, and U. H. L. Hsu, "Theory and Application of Calibration Techniques for a NDBC Directional Wave Measurements Buoy," *IEEE J. Oceanic Eng.* **OE-10**, 382-396 (1985).

[3] M. S. Longuet-Higgins, D. E. Cartwright, and N. D. Smith, "Observations of the Directional Spectrum of Sea Waves Using the Motions of a Floating Buoy," in *Ocean Wave Spectra*, Prentice Hall, Englewood Cliffs, N.J., pp. 111-136 (1963).

[4] E. J. Walsh, D. W. Hancock III, D. E. Hines, R. N. Swift, and J. F. Scott, "Elimination of Directional Wave Spectrum Contamination from Noise in Elevation Measurements," *IEEE J. Oceanic Eng.* **OE-10**, 376-381 (1985).

[5] F. C. Jackson, W. T. Walton, and P. L. Baker, "Aircraft and Satellite Measurements of Ocean Wave Directional Spectra Using Scanning-Beam Microwave Radars," *J. Geophys. Res.* **90**, 987-1004 (1985).

[6] F. C. Jackson, W. T. Walton, and C. Y. Peng, "A Comparison of in situ and Airborne Radar Observations of Ocean Wave Directionality," *J. Geophys. Res.* **90**, 1005-1018 (1985).

[7] R. C. Beal, T. W. Gerling, D. E. Irvine, F. M. Monaldo, and D. G. Tilley, "Spatial Variations of Ocean Wave Directional Spectra from the SEASAT Synthetic Aperture Radar," *J. Geophys. Res.* **91**, 2433-2449 (1986).

[8] D. E. Cartwright, "The Use of Directional Spectra in Studying the Output of a Wave Recorder on a Moving Ship," in *Ocean Wave Spectra*, Prentice Hall, Englewood Cliffs, N.J., pp. 203-207 (1963).

[9] H. Mitsuyasu, Y. Y. Kuo, and A. Masuda, "On the Dispersion Relation of Random Gravity Waves. Part 2. An Experiment," *J. Fluid Mech.* **92**, 731-749 (1979).

[10] M. A. Donelan, J. Hamilton, and W. H. Hui, "Directional Spectra of Wind-Generated Waves," *Phil. Trans. R. Soc. London* **A315**, 509-562 (1985).

[11] R. B. Long and K. Hasselmann, "A Variational Technique for Extracting Directional Spectra from Multicomponent Wave Data," *J. Phys. Oceanogr.* **9**, 373-381 (1979).

[12] R. B. Long, "The Statistical Evaluation of Directional Spectrum Estimates Derived from Pitch and Roll Buoy Data," *J. Phys. Oceanogr.* **10**, 944-952 (1980).

[13] G. Neumann and W. J. Pierson, *Principles of Physical Oceanography*, Prentice Hall, Englewood Cliffs, N.J. (1966).

[14] J. W. Tukey, "The Sampling Theory of Power Spectrum Estimates," presented at Symp. on Applications of Autocorrelation Analysis to Physical Problems, Woods Hole, Mass. (Jun 13, 1949).

[15] R. B. Blackman and J. W. Tukey, "The Measurement of Power Spectra from the Point of View of Communications Engineering," *Bell Syst. Tech. J.* **XXXVII** (1958). (Reprinted, Dover Pubs., New York (1959)).

[16] F. J. Harris, "On the Use of Windows for Harmonic Analysis with the Discrete Fourier Transform," *Proc. IEEE* **64**, 51-83 (1978).

[17] J. W. Cooley and J. W. Tukey, "An Algorithm for the Machine Calculation of Complex Fourier Series," *Math. Comput.* **19**, 297-307 (1965).

[18] N. R. Goodman, "Spectral Analysis of Multiple Stationary Time Series," in *Time Series Analysis*, Wiley, New York, pp. 260-265 (1963).

[19] W. H. Munk, "Ocean Waves as a Meteorological Tool," in *Compendium of Meteorology*, T. F. Malone, ed., American Meteorological Society, Boston, pp. 1090-1100 (1951).

[20] W. J. Pierson, "Comments on 'A Parametric Wave Prediction Model'," *J. Phys. Oceanogr.* **7**, 127-134 (1977).

[21] S. F. Barstow, G. Ueland, and B. A. Fossum, "The WAVESCAN Second Generation Directional Wave Buoy," presented at Oceanology International Conf., Brighton, U.K. (1986).

[22] H. Mitsuyasu, F. Tasai, T. Suhara, S. Mizuno, M. Ohkuso, T. Honda, and K. Rikiishi, "Observations of the Directional Spectrum of Ocean Waves Using a Cloverleaf Buoy," *J. Phys. Oceanogr.* **5**, 750-760 (1975).

[23] L. M. Lawson and R. B. Long, "Multimodel Properties of the Surface Wave Field Observed with Pitch-Roll Buoys during GATE," *J. Phys. Oceanogr.* **13**, 3 (1983).

ACKNOWLEDGMENTS—The support of the National Data Buoy Center for this research by means of Contract 40-QANW-5-00261M.3 is acknowledged. K. E. Steele provided invaluable help in many conversations concerning the methods presently in use for the analysis of buoy data. This article is based on a study by the author for NDBC. Copies can be obtained on request.